OPTIMAL MULTIREVOLUTIONAL TRANSFERS BETWEEN NON-COPLANAR ELLIPTICAL ORBITS

Vyacheslav PETUKHOV

Khrunichev State Research & Production Space Center

Novozavodskaja st., 18, Moscow, 121087, Russia. E-mail : petukhov@mtu-net.ru

ABSTRACT : It is considered optimization of low-thrust trajectories between non-coplanar elliptical orbits. The optimal control problem is reduced to the two-point boundary value problem (TPBVP) by means of maximum principle. The numerical homotopic technique and modified newton technique are used to solve TPBVP. Differential equations of optimal motion are numerically averaged when TPBVP is solved. It was developed the robust and efficient software and a large number of optimal trajectories were calculated. New qualitative results were obtained. In particularity, there were found bifurcation of optimal solutions and existence of the critical initial inclination. The partial classification of optimal control structure was carried out.

1 - PROBLEM DEFINITION

It is considered optimization of low-thrust transfer between non-coplanar elliptical orbits in the inverse square low field. Significance of this problem is connected with planned using of electric propulsion for advanced spacecraft insertion. The advanced missions includes low-thrust insertion into GEO [1-3, 5-11], satellite systems forming and maintenance, spiral untwisting around the Earth for spacecraft insertion into an escape trajectory [4, 10, 11-14].

Optimization problem of low-thrust transfer between non-coplanar elliptical orbits reduces to the two-point boundary value problem (TPBVP) by means of Pontryagin's maximum principle. Difficulty of solving the TPBVP is connected, in particular, with problem of initial guess value, which is caused by complex topology of optimal solution in the parametric space. Optimal solutions bifurcations lead to the discontinuity of TBVP residual vector's derivative with respect to initial value of TBVP parameters during crossing bounds of regions having different solutions (i.e. hypersurfaces having singular sensitivity matrix). This leads to the failure or instability of numerical methods.

Characteristic features of electric propulsion transfers are defined mainly by a low thrust-to-gravity force ratio. Thrust acceleration smallness leads to the long-duration transfers. The typical low-thrust transfer to GEO includes hundreds orbits. In this case, the differential equations of optimal motion becomes very sensitive with respect to variations of initial values of co-state variables. This sensitivity makes still more difficult the TPBVP solving. In this circumstances, insufficient number of digits in the machine representation of real number becomes one of the practical barrier for the numerical solving the optimal control problem. Another problem is essential increase of requirements to the computational productivity when it increases the number of trajectory revolutions.

The averaging technique [1-3, 8, 9, 11] is used to decrease differential equations instability and computational consumption. If optimal control structure is pre-fixed, then maximum principle is applied to the averaged equations for optimization of slow control parameters. However, the best results are obtained by another approach, when optimality conditions are derived from the non-averaged equations and then these optimal equations are averaged. Equation of motion are presented in the Keplerian elements. The numerical averaging over the orbit is used and a version of modified newton or shooting method is used to solve corresponding TPBVP.

We will consider optimal transfers between non-coplanar elliptic orbits for a minimum or fixed time. The numerical algorithm based on continuation technique [11-13] is described. There are analyzed features of optimal trajectories, in particularity, transfer trajectories from the inclined circular or elliptical orbits to GEO.

2 - EQUATIONS OF MOTION

Let us consider spacecraft motion under the influence of the primary gravity force and electric propulsion thrust. Magnitudes of the thrust and specific impulse of running electric propulsion engine are assumed to be constant. There are not applied any constraints to the thrust attitude. Gravity force is assumed to be obeyed to the inverse square law.

Thrust acceleration projections into orbital orts are following:

$$a_t = \boldsymbol{d}\frac{P}{m}\cos \boldsymbol{J}\cos \boldsymbol{y}\ ,\ a_r = \boldsymbol{d}\frac{P}{m}\sin \boldsymbol{J}\cos \boldsymbol{y}\ ,\ a_n = \boldsymbol{d}\frac{P}{m}\sin \boldsymbol{y}\ , \tag{1}$$

where a_t, a_r, a_n – transversal, radial, and binormal projection of thrust acceleration correspondingly, $\boldsymbol{d}$ - thrust step function ($\boldsymbol{d}$=1 if engine is running, and $\boldsymbol{d}$=0 if engine is switched off), P – thrust magnitude, m – spacecraft mass, $\boldsymbol{J}$ - «pitch» angle (angle between projection of thrust vector onto the orbital plane and transversal), $\boldsymbol{y}$ - «yaw» angle (angle between thrust vector and orbital plane).

To avoid singularity in the vicinity of zero eccentricity and inclination, there are used equations of motion in the equinoctial elements [1]:

$$\left.\begin{aligned}
\frac{dh}{dt} &= \boldsymbol{d}\frac{P}{m}\frac{h}{\boldsymbol{x}}\cdot h\cos \boldsymbol{J}\cos \boldsymbol{y},\\
\frac{de_x}{dt} &= \boldsymbol{d}\frac{P}{m}\frac{h}{\boldsymbol{x}}\left\{\boldsymbol{x}\sin F\sin \boldsymbol{J}\cos \boldsymbol{y} + \left[(\boldsymbol{x}+1)\cos F + e_x\right]\cos \boldsymbol{J}\cos \boldsymbol{y} - e_y \boldsymbol{h}\sin \boldsymbol{y}\right\},\\
\frac{de_y}{dt} &= \boldsymbol{d}\frac{P}{m}\frac{h}{\boldsymbol{x}}\left\{-\boldsymbol{x}\cos F\sin \boldsymbol{J}\cos \boldsymbol{y} + \left[(\boldsymbol{x}+1)\sin F + e_y\right]\cos \boldsymbol{J}\cos \boldsymbol{y} + e_x \boldsymbol{h}\sin \boldsymbol{y}\right\},\\
\frac{di_x}{dt} &= \boldsymbol{d}\frac{P}{m}\frac{h}{\boldsymbol{x}}\cdot\frac{1}{2}\tilde{\boldsymbol{j}}\cos F\sin \boldsymbol{y},\\
\frac{di_y}{dt} &= \boldsymbol{d}\frac{P}{m}\frac{h}{\boldsymbol{x}}\cdot\frac{1}{2}\tilde{\boldsymbol{j}}\sin F\sin \boldsymbol{y},\\
\frac{dF}{dt} &= \frac{\boldsymbol{x}^2}{h^3} + \boldsymbol{d}\frac{P}{m}\frac{h}{\boldsymbol{x}}\cdot \boldsymbol{x}\boldsymbol{h}\sin \boldsymbol{y},\\
\frac{dm}{dt} &= -\boldsymbol{d}\frac{P}{w},
\end{aligned}\right\} \tag{2}$$

where $h=\sqrt{\dfrac{p}{m}}$, $e_x = e\cos(\Omega + \boldsymbol{w})$, $e_y = e\sin(\Omega + \boldsymbol{w})$, $i_x = \tan\dfrac{i}{2}\cos\Omega$, $i_y = \tan\dfrac{i}{2}\sin\Omega$, and $F = \boldsymbol{n} + \boldsymbol{w} + \Omega$ - equinoctial elements, p – semi-latus rectum, e – eccentricity, $\boldsymbol{w}$ - argument of pericentre, i – inclination, Ω - right ascension of ascending node, $\boldsymbol{n}$ - true anomaly, $\boldsymbol{x} = 1 + e_x\cos F + e_y\sin F$, $\boldsymbol{h} = i_x\sin F - i_y\cos F$, $\tilde{\boldsymbol{j}} = 1 + i_x^2 + i_y^2$, w – exhaust velocity of electric propulsion.

It is necessary to transfer spacecraft having initial mass m_0 from the initial orbit

$$h=h_0,\ e_x=e_{x0},\ e_y=e_{y0},\ i_x=i_{x0},\ i_y=i_{y0} \tag{3}$$

into the final one

$$h=h_k,\ e_x=e_{xk},\ e_y=e_{yk},\ i_x=i_{xk},\ i_y=i_{yk} \tag{4}$$

for a time T.

It is considered the minimization of performance index

$$J = \int_0^T \boldsymbol{d}\frac{P}{w}dt \to \min\ , \tag{5}$$

which corresponds to the minimum-propellant problem. If there are not a constraints on transfer duration T and if $\boldsymbol{d} \equiv 1$, performance index (5) corresponds to the minimum-time problem. However, the more conventional performance index for a minimum-time problem is

$$J = \int_0^T dt \to \min\ . \tag{5a}$$

Within a problem of transfer between orbits for a minimum time, the difference between performance indices (5) è (5a) is reduced to the different normalization of adjoint vector by means of transversality conditions.

3 - OPTIMAL CONTROL

The maximum principle is used to solve the problem (2-5). The Hamiltonian of optimal control problem (2-5) is

$$H = -\boldsymbol{d}\frac{P}{w}(1+p_m) + \frac{\boldsymbol{x}^2}{h^3}p_F + \boldsymbol{d}\frac{P}{m}\frac{h}{\boldsymbol{x}}\left(A_t\cos\boldsymbol{J}\cos\boldsymbol{y} + A_r\sin\boldsymbol{J}\cos\boldsymbol{y} + A_n\sin\boldsymbol{y}\right) \tag{6}$$

where

$$A_t = hp_h + \left[(\boldsymbol{x}+1)\cos F + e_x\right]p_{ex} + \left[(\boldsymbol{x}+1)\sin F + e_y\right]p_{ey}\ ,$$

$$A_r = \boldsymbol{x}\left(\sin F\cdot p_{ex} - \cos F\cdot p_{ey}\right),$$

$$A_n = \boldsymbol{h}\left(-e_y p_{ex} + e_x p_{ey}\right) + \frac{1}{2}\tilde{\boldsymbol{j}}\left(\cos F\cdot p_{ix} + \sin F\cdot p_{iy}\right) + \boldsymbol{x}\boldsymbol{h}\cdot p_F\ ,$$

p_h, p_{ex}, p_{ey}, p_{ix}, p_{iy}, p_F, p_m –adjoint variables, coupled with the phase coordinates h, e_x, e_y, i_x, i_y, F, and m correspondingly.

Optimal controls $\boldsymbol{d}(t)$, $\boldsymbol{J}(t)$, $\boldsymbol{y}(t)$ are defined from the Hamiltonian (6) maximization:

$$\cos J = \frac{A_t}{\sqrt{A_t^2 + A_r^2}},\ \sin J = \frac{A_r}{\sqrt{A_t^2 + A_r^2}}, \tag{7}$$

$$\cos y = \frac{\sqrt{A_t^2 + A_r^2}}{\sqrt{A_t^2 + A_r^2 + A_n^2}},\ \sin y = \frac{A_n^2}{\sqrt{A_t^2 + A_r^2 + A_n^2}}, \tag{8}$$

$$d = \begin{cases} 1, y_s > 0 \\ 0, y_s \le 0, \end{cases} \tag{9}$$

where $y_s = -\frac{1+p_m}{w} + \frac{h}{mx}\left(A_t^2 + A_r^2 + A_n^2\right)^{1/2}$ - switching function. Within the minimum-time problem, the identity

$$d \equiv 1, \tag{10}$$

is used instead of (9), and differential equations for m and p_m can be eliminated using explicit expression for the spacecraft mass:

$$m = m_0 - (P/w)\cdot t\,. \tag{11}$$

Substitution of (7), (8), and (9) or (10) into (6) leads to the expression for the optimal Hamiltonian:

$$H = dP\left[\frac{1}{m}\frac{h}{x}\left(A_t^2 + A_r^2 + A_n^2\right)^{1/2} - \frac{1+p_m}{w}\right] + \frac{x^2}{h^3}p_F = dP[kA+b] + H_F\,, \tag{12}$$

where $k = \frac{1}{m}\frac{h}{x}$, $A = \left(A_t^2 + A_r^2 + A_n^2\right)^{1/2}$, $b = -\frac{1+p_m}{w}$, $H_F = \frac{x^2}{h^3}p_F$.

The equations of optimal motions become following:

$$\left.\begin{aligned}
\frac{d\mathbf{x}}{dt} &= \frac{\partial H}{\partial \mathbf{p}} = dP\left[k\left(A_t\frac{\partial A_t}{\partial \mathbf{p}} + A_r\frac{\partial A_r}{\partial \mathbf{p}} + A_n\frac{\partial A_n}{\partial \mathbf{p}}\right)A^{-1}\right],\\
\frac{dF}{dt} &= \frac{\partial H}{\partial p_F} = dP\left[k\left(A_t\frac{\partial A_t}{\partial p_F} + A_r\frac{\partial A_r}{\partial p_F} + A_n\frac{\partial A_n}{\partial p_F}\right)A^{-1}\right] + \frac{\partial H_F}{\partial p_F},\\
\frac{dm}{dt} &= \frac{\partial H}{\partial p_m} = dP\frac{\partial b}{\partial p_m},\\
\frac{d\mathbf{p}}{dt} &= -\frac{\partial H}{\partial \mathbf{x}} = -dP\left[\frac{\partial k}{\partial \mathbf{x}}A + k\left(A_t\frac{\partial A_t}{\partial \mathbf{x}} + A_r\frac{\partial A_r}{\partial \mathbf{x}} + A_n\frac{\partial A_n}{\partial \mathbf{x}}\right)A^{-1}\right] - \frac{\partial H_F}{\partial \mathbf{x}},\\
\frac{dp_F}{dt} &= -\frac{\partial H}{\partial F} = -dP\left[\frac{\partial k}{\partial F}A + k\left(A_t\frac{\partial A_t}{\partial F} + A_r\frac{\partial A_r}{\partial F} + A_n\frac{\partial A_n}{\partial F}\right)A^{-1}\right] - \frac{\partial H_F}{\partial F},\\
\frac{dp_m}{dt} &= -\frac{\partial H}{\partial m} = -dP\frac{\partial k}{\partial m}A.
\end{aligned}\right\} \tag{13}$$

where $\mathbf{x} = \left(h, e_x, e_y, i_x, i_y\right)^{\mathrm{T}}, \mathbf{p} = \left(p_h, p_{ex}, p_{ey}, p_{ix}, p_{iy}\right)^{\mathrm{T}}$.

Since the transfer between orbits is considered, the final true longitude F is not fixed, therefore $p_F(T)=0$. The optimal Hamiltonian does not depend on F after averaging, therefore $\frac{dp_F}{dt} = -\frac{\partial H}{\partial F} = 0$. So, $p_F \equiv 0$ on the averaged solution. The optimal Hamiltonian, taking into account supposed averaging, becomes following:

$$H = \delta P[kA + b], \tag{14}$$

and the equations of motion (13) can be rewritten in the form:

$$\left.\begin{aligned}
\frac{d\mathbf{x}}{dt} &= \frac{\partial H}{\partial \mathbf{p}} = \delta P\left[k\left(A_t\frac{\partial A_t}{\partial \mathbf{p}} + A_r\frac{\partial A_r}{\partial \mathbf{p}} + A_n\frac{\partial A_n}{\partial \mathbf{p}}\right)A^{-1}\right],\\
\frac{dm}{dt} &= \frac{\partial H}{\partial p_m} = \delta P\frac{\partial b}{\partial p_m},\\
\frac{d\mathbf{p}}{dt} &= -\frac{\partial H}{\partial \mathbf{x}} = -\delta P\left[\frac{\partial k}{\partial \mathbf{x}}A + k\left(A_t\frac{\partial A_t}{\partial \mathbf{x}} + A_r\frac{\partial A_r}{\partial \mathbf{x}} + A_n\frac{\partial A_n}{\partial \mathbf{x}}\right)A^{-1}\right],\\
\frac{dp_m}{dt} &= -\frac{\partial H}{\partial m} = -\delta P\frac{\partial k}{\partial m}A.
\end{aligned}\right\} \tag{15}$$

In case of minimum-time problem δ≡1, $m = m_0 - \frac{P}{w}t$, so equations for m è p_m can be eliminated:

$$\left.\begin{aligned}
\frac{d\mathbf{x}}{dt} &= \frac{\partial H}{\partial \mathbf{p}} = \delta P\left[k\left(A_t\frac{\partial A_t}{\partial \mathbf{p}} + A_r\frac{\partial A_r}{\partial \mathbf{p}} + A_n\frac{\partial A_n}{\partial \mathbf{p}}\right)A^{-1}\right],\\
\frac{d\mathbf{p}}{dt} &= -\frac{\partial H}{\partial \mathbf{x}} = -\delta P\left[\frac{\partial k}{\partial \mathbf{x}}A + k\left(A_t\frac{\partial A_t}{\partial \mathbf{x}} + A_r\frac{\partial A_r}{\partial \mathbf{x}} + A_n\frac{\partial A_n}{\partial \mathbf{x}}\right)A^{-1}\right]
\end{aligned}\right\} \tag{15a}$$

4 - AVERAGING

Low thrust-to-gravity acceleration ratio allows to use averaging of optimal differential equations. The averaging allows to increase the integration step size and, therefore, to decrease computational consumptions. But main reason of averaging usage is its regularizing role: the averaged differential equations are more stable numerically in comparison with non-averaged ones.

The averaging on time over the spacecraft orbital period is used. It is equivalent to well-known in celestial mechanics averaging on mean anomaly. The asymptotic basis of the averaging is well-known too: solution of averaged differential equations is zero-order term of the Fourier series expansion of non-averaged solution. The intuitive basis of the averaging is confined in the smallness variation of the slow orbital elements during one revolution due to low thrust.

Differential equations are averaged using following expression:

$$\frac{d\mathbf{y}}{dt} = \frac{1}{T}\int_{t_0}^{t_0+T}\mathbf{f}(\mathbf{y},F,t)dt = \frac{n}{2\pi}\int_0^{2\pi}\mathbf{f}(\mathbf{y},F,t)\frac{dt}{dF}dF, \tag{16}$$

where $\mathbf{y}=(\mathbf{x}^{\mathrm{T}}, \mathbf{p}^{\mathrm{T}})^{\mathrm{T}}$ for minimum-time problem, $\mathbf{y}=(\mathbf{x}^{\mathrm{T}}, m, \mathbf{p}^{\mathrm{T}}, p_m)^{\mathrm{T}}$ for minimum-propellant problem, $\mathbf{f}(\mathbf{y},F,t)$ – the right parts of non-averaged differential equations (15) or (15a), $n = \frac{1}{m}\left[\sqrt{1-e_x^2-e_y^2}\big/h\right]^3$ - mean motion, $dt/dF = h^3/x^2$.

5 - BOUNDARY VALUE PROBLEM AND TRANSVERSALITY CONDITIONS

State vector **x**, co-state vector **p**, and residual vector **f** at the final time T are computed as result of integration of equations (15) or (15a) using averaging (16). Residual vector is following:

$$\mathbf{f} = \begin{pmatrix} h(T) - h_k \\ e_x(T) - e_{xk} \\ e_y(T) - e_{yk} \\ i_x(T) - i_{xk} \\ i_y(T) - i_{yk} \\ p_m(T) \end{pmatrix} = 0 \tag{17}$$

for the fixed time (minimum-propellant) problem and

$$\mathbf{f} = \begin{pmatrix} h(T) - h_k \\ e_x(T) - e_{xk} \\ e_y(T) - e_{yk} \\ i_x(T) - i_{xk} \\ i_y(T) - i_{yk} \\ H(T) \end{pmatrix} = 0 \tag{17a}$$

for the minimum-time problem.

It is necessary to solve equations (17), (17a) with respect to vector of unknown TPBVP parameters **z**. Vector **z** has form:

$$\mathbf{z} = \begin{pmatrix} \mathbf{p} \\ p_m \end{pmatrix} \tag{18}$$

for minimum-propellant problem

$$\mathbf{z} = \begin{pmatrix} \mathbf{p} \\ T \end{pmatrix} \tag{18a}$$

for minimum-time problem.

Let us consider different kinds of boundary conditions.

5.1 - FINAL SPACECRAFT MASS IS GIVEN IN THE MINIMUM-PROPELLANT PROBLEM.

It is necessary to find initial mass of spacecraft m_0, which becomes 7^{th} parameter of the TPBVP instead of p_m in the equation (18). The transversality condition $p_m(0)=0$ should be satisfied at the initial time, and the condition $m(T)-m_k=0$ instead of $p_m(T)=0$ should be included in the equation (17).

5.2 - FREE PERICENTRE RADIUS.

There are given apocenter radius r_{ak}, argument of pericentre w_k, inclination i_k, and right ascension of ascending node Ω_k for the final orbit. In the equinoctial elements these conditions have form:

$$\mathbf{g}(T) = \begin{pmatrix} mh^2 - r_{ak}\left(1 - \sqrt{e_x^2 + e_y^2}\right) \\ \left(e_x i_x + e_y i_y\right)\sin w_k - \left(e_y i_x - e_x i_y\right)\cos w_k \\ i_x - \tan\frac{i_k}{2}\cos\Omega_k \\ i_y - \tan\frac{i_k}{2}\sin\Omega_k \end{pmatrix} = 0\,. \tag{19}$$

Transversality conditions are expressed from the equations:

$$
\left.
\begin{aligned}
p_h(T) &= \boldsymbol{n}_1 \frac{\partial g_1}{\partial h}, \\
p_{ex}(T) &= \boldsymbol{n}_1 \frac{\partial g_1}{\partial e_x} + \boldsymbol{n}_2 \frac{\partial g_2}{\partial e_x}, \\
p_{ey}(T) &= \boldsymbol{n}_1 \frac{\partial g_1}{\partial e_y} + \boldsymbol{n}_2 \frac{\partial g_2}{\partial e_y}, \\
p_{ix}(T) &= \boldsymbol{n}_2 \frac{\partial g_2}{\partial i_x} + \boldsymbol{n}_3, \\
p_{iy}(T) &= \boldsymbol{n}_2 \frac{\partial g_2}{\partial i_y} + \boldsymbol{n}_4
\end{aligned}
\right\} \tag{20}
$$

after exclusion from this system the undetermined multipliers $\boldsymbol{n}_i$. As it follows from (20), the final magnitudes of p_{ix} and p_{iy} are an constraint-free, so it is sufficient to consider the 3 first equations of system (20). Let us exclude $\boldsymbol{n}_2$ from the 2^nd and 3^rd equations. Then let us substitute the expression for $\boldsymbol{n}_1$, which is getting from the 1^st equation, into the derived equation. Finally, we will get following transversality condition:

$$
\begin{aligned}
&\left[2(1-e)ep_{ex} - p_h he_x\right]\left(i_y \sin \boldsymbol{w}_k - i_x \cos \boldsymbol{w}_k\right) - \\
&- \left[2(1-e)ep_{ey} - p_h he_y\right]\left(i_x \sin \boldsymbol{w}_k + i_y \cos \boldsymbol{w}_k\right) = 0,
\end{aligned} \tag{21}
$$

where $e = \sqrt{e_x^2 + e_y^2}$ - eccentricity. Equation (21), equations (19), and corresponding condition for $p_m(T)$ or $m_k(T)$ are enclose the system of boundary conditions at the final time.

5.3 - FREE APOCENTER RADIUS.

Case of free apocenter radius is similar to case of free pericentre radius, but the 1^st equation in the (19) should be replaced by

$$
g_1(T) = mh^2 - r_{pk}\left(1 + \sqrt{e_x^2 + e_y^2}\right) = 0\,, \tag{22}
$$

where r_{pk} – given final pericentre radius. The corresponding transversality condition becomes following:

$$
\begin{aligned}
&\left[2(1+e)ep_{ex} - p_h he_x\right]\left(i_y \sin \boldsymbol{w}_k - i_x \cos \boldsymbol{w}_k\right) - \\
&- \left[2(1+e)ep_{ey} - p_h he_y\right]\left(i_x \sin \boldsymbol{w}_k + i_y \cos \boldsymbol{w}_k\right) = 0.
\end{aligned} \tag{23}
$$

5.4 - FREE LINES OF APSIDES AND NODES.

If lines of apsides and nodes of final orbit are free, then following conditions should be satisfied at the final time:

$$
\mathbf{g}(T) = \begin{pmatrix} h - h_k \\ e_x^2 + e_y^2 - e_k^2 \\ i_x^2 + i_y^2 - \tan^2 \dfrac{i_k}{2} \end{pmatrix} = 0. \tag{24}
$$

Additional transversality condition are following:

$$\left.\begin{aligned} p_{ex}e_y - p_{ey}e_x &= 0, \\ p_{ix}i_y - p_{iy}i_x &= 0. \end{aligned}\right\} \tag{25}$$

5.5 - FREE LINE OF NODES.

Free final line of nodes corresponds to the following conditions at the final time:

$$\mathbf{g}(T) = \begin{pmatrix} h - h_k \\ e_x^2 + e_y^2 - e_k^2 \\ \left(e_x i_x + e_y i_y\right)\sin w_k - \left(e_y i_x - e_x i_y\right)\cos w_k \\ i_x^2 + i_y^2 - \tan^2 \dfrac{i_k}{2} \end{pmatrix} = 0. \tag{26}$$

In addition, the transversality conditions should be satisfied

$$\begin{aligned} &\left(p_{ix}i_y - p_{iy}i_x + p_{ex}e_y - p_{ey}e_x\right)\cos(w - w_k) = 0 \Leftrightarrow \\ &p_{ix}i_y - p_{iy}i_x + p_{ex}e_y - p_{ey}e_x = 0. \end{aligned} \tag{27}$$

5.6 - FREE LINE OF APSIDES.

If initial argument of pericentre is free, then final boundary conditions are following:

$$\mathbf{g}(T) = \begin{pmatrix} h - h_k \\ e_x^2 + e_y^2 - e_k^2 \\ i_x - i_{xk} \\ i_y - i_{yk} \end{pmatrix} = 0, \tag{28}$$

and transversality condition is following:

$$p_{ex}e_y - p_{ey}e_x = 0. \tag{29}$$

5.7 - IT IS FIXED ONLY APOCENTER OR PERICENTRE RADIUS.

In this case boundary condition at the final time is following:

$$g(T) = mh^2 - r_k\left(1 \mp \sqrt{e_x^2 + e_y^2}\right) = 0\,, \tag{30}$$

where r_k – the fixed apocenter radius or pericentre radius of final orbit, sign «-» corresponds to fixed apocenter radius, and sign «+» corresponds to the fixed pericentre radius. Expression (30) leads to the following transversality conditions:

$$\left.\begin{aligned} 2mehp_{ex} \mp r_k e_x p_h &= 0, \\ 2mehp_{ey} \mp r_k e_y p_h &= 0, \\ p_{ix} &= 0, \\ p_{iy} &= 0. \end{aligned}\right\} \tag{31}$$

5.8 - FREE PERICENTRE OR APOCENTER RADIUS AND FREE LINE OF APSIDES.

The boundary conditions at the final time are following:

$$\mathbf{g}(T) = \begin{pmatrix} mh^2 - r_k\left(1 \mp \sqrt{e_x^2 + e_y^2}\right) \\ e_x^2 + e_y^2 - e_k^2 \\ i_x - i_{xk} \\ i_y - i_{yk} \end{pmatrix} = 0, \quad (32)$$

where r_k and signs are the same as in the previous considered case. In addition to (32), the following transversality condition should be satisfied at the final time:

$$p_{ex}e_y - p_{ey}e_x = 0. \quad (33)$$

5.9 - FIXED SEMI-LATUS RECTUM.

In this case boundary condition at the final time is following:

$$g(T) = mh^2 - p_k, \quad (34)$$

where p_k – fixed final semi-latus rectum. Expression (34) should be completed by trivial transversality conditions:

$$\left.\begin{aligned} p_{ex}(T) &= 0, \\ p_{ey}(T) &= 0, \\ p_{ix}(T) &= 0, \\ p_{iy}(T) &= 0. \end{aligned}\right\} \quad (35)$$

5.10 - FIXED SEMIMAJOR AXIS.

In this case boundary condition at the final time is following:

$$g(T) = \frac{mh^2}{1 - e_x^2 - e_y^2} - a_k, \quad (36)$$

where a_k – fixed final semimajor axis. Expression (36) should be completed by following transversality conditions at $t = T$:

$$\left.\begin{aligned} p_{ex}\left(1 - e_x^2 - e_y^2\right) - p_h h e_x &= 0, \\ p_{ey}\left(1 - e_x^2 - e_y^2\right) - p_h h e_y &= 0, \\ p_{ix} &= 0, \\ p_{iy} &= 0. \end{aligned}\right\} \quad (37)$$

6 - TECHNIQUES OF THE BOUNDARY VALUE PROBLEM SOLVING

The boundary value problem solving is reduced to the solving of nonlinear system, which is consisted of a state residuals and a transversality conditions. The continuations technique or versions of modified newton methods were used to solve this system. The continuation method belongs to the class of homotopic methods. One of the most simple version of continuation method was used in this study. The original problem is immersed into some one-parametric family and then it is used the linear continuation of the problem solution with respect to the family parameter.

The essence of considered continuation technique is following. Let it is necessary to solve the nonlinear system

$$\mathbf{f}(\mathbf{z})=0. \tag{34}$$

Let $\mathbf{f}(\mathbf{z}_0)=\mathbf{b}$ at some initial approximation $\mathbf{z}_0$. Let us consider following one-parametric nonlinear system

$$\mathbf{f}_1(\mathbf{z},\tau)=\mathbf{f}(\mathbf{z})-(1-\tau)\mathbf{b}=0. \tag{35}$$

When $\tau=0$, $\mathbf{z}=\mathbf{z}_0$

$$\mathbf{f}_1(\mathbf{z}_0,\tau)=0, \tag{36}$$

and when $\tau=1$ $\mathbf{f}_1(\mathbf{z},\tau)=\mathbf{f}(\mathbf{z})$. Let us represent the solution of problem (35) as function of continuation parameter τ: $\mathbf{z}=\mathbf{z}(\tau)$. By virtue of (35), (36), $\mathbf{z}(\tau)$ can be represented as solution of the following system of ordinary differential equations:

$$\frac{d\mathbf{z}}{dt}=-\left[\frac{\partial\mathbf{f}(\mathbf{z})}{\partial\mathbf{z}}\right]^{-1}\mathbf{b} \tag{37}$$

having following initial condition:

$$\mathbf{z}(0)=\mathbf{z}_0. \tag{38}$$

After integrating the system (37), (38) on τ from 0 to 1, we get solution of the original problem (34). Thus, the solving of nonlinear system (34) is reduced formally to the initial value problem (37), (38). The system (37) we will name the differential equations system of continuation method.

If Euler method is used for problem (37), (38) integration, then the continuation method converts to the classical newton method. The advantage of continuation method in comparison with newton method appears if more advanced numerical integrators are used. If an ideal integration method is used, then the convergence domain of the continuation method in the parametric space $\mathbf{z}$ is coincided with the attraction area of given solution in this space. Equations (37) have singularity on the hypersurface where matrix $\partial\mathbf{f}/\partial\mathbf{z}$ is singular, therefore continuation method (as newton methods) is failed during crossing these hypersurfaces. Singularity of $\partial\mathbf{f}/\partial\mathbf{z}$ generally take place on the bounds of the attraction region of solution. The singularity is connected with a solution bifurcation of the original system (34).

Right parts of equations (15) or (15a) are numerically averaged using expression (16) during integration corresponding system. The simple numerical techniques were used to get the integrals of functions. There are method of trapezoids or Simpson's method on the fixed uniform grid on F consisting of 30-300 nodes. The explicit Runge-Kutta method of 7^{th} (8^{th}) order was used to integrate the averaging system (15). The initial conditions of basic problem were following:

$$\left.\begin{aligned}&h=h_0,e_x=e_{x0},e_y=e_{y0},i_x=i_{x0},i_y=i_{y0},m=m_0,\\&p_h=p_{h0},p_{ex}=p_{ex0},p_{ey}=p_{ey0},p_{ix}=p_{ix0},p_{iy}=p_{iy0},p_m=p_{m0}\end{aligned}\right\} \tag{39}$$

at the $t=0$. For minimum-time problem the spacecraft mass is parameter, so conditions for mass and for adjoint to mass variables should be excluded from (39).

The continuation technique demonstrated its highly effectiveness for solving minimum-time problems. In most problems, the convergence to the optimal solution was achieved by choice the following initial approximation for TPBVP parameters vector:

$$p_h=1,\ p_{ex}=p_{ey}=p_{ix}=p_{iy}=0,\ T=1,$$

where T – dimensionless time referred to the initial orbit. When parameters of the initial or final orbit were varied, the TPBVP parameters vector of previous problem was used as initial approximation.

Unfortunately, the continuation technique was found insufficiently efficient for the minimum-propellant problem. The modified newton method was used in this case, and TPBVP parameters vector of corresponding minimum-time problem was used as initial approximation.

7 - NUMERICAL RESULTS.

7.1 - TRANSFER BETWEEN CIRCULAR NON-COPLANAR ORBITS.

At first, let us consider the most simple problem – the minimum-time transfer between circular non-coplanar orbits. Within all model problems we will use the same spacecraft parameters:

- initial mass of spacecraft is 1320 kg;
- electric propulsion thrust is 0.332 N;
- electric propulsion specific impulse is 1500 s.

Trajectory perturbations due to Earth oblateness, Moon, Sun, and planets gravity forces, impact of eclipses and solar array degradation are not took into account.

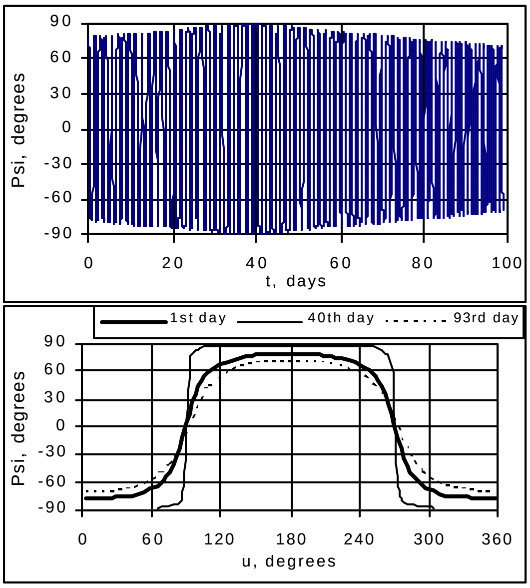

Fig. 1. Dependency of angle ψ vs. time and argument of latitude for transfer from circular orbit h = 45000 km, i = 30° into the GEO

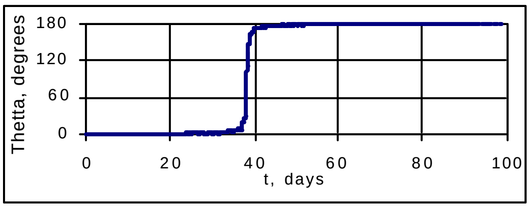

Fig. 2. Dependency of angle ϑ vs. time for transfer from circular orbit h = 45000 km, i = 30° into the GEO

The series computations of optimal transfers from the circular orbits, having different altitude and inclination, into the GEO was carried out using developed techniques and software. Analysis of obtained numerical data leads to the interesting new result: the bifurcation of an optimal solution and the critical initial inclination are exist. If inclination is less critical one ($i_{cr} \approx 47.3°$) then exists unique solution of the minimum-time problem. The thrust vector is always orthogonal to the spacecraft radius-vector on this solution, and eccentricity is identically equals to zero. Thrust steering is restricted by controlling of angle y between thrust vector and orbital plane in this case. An example of dependency of angle y with respect to time and argument of latitude is presented in the Fig. 1.

Maximal absolute magnitude of angle y on the orbit y_{max} is reached in the nodal points. Angle y_{max} increases when time increases and it reaches maximal magnitude 90° when the semimajor axis reaches its maximal magnitude. Then y_{max} decreases.

The typical situation on these solution is acceleration during initial transfer phase (phase of increasing y_{max}) and braking during final transfer phase (phase of decreasing y_{max}). The typical dependency of angle J (angle between projection of the thrust vector onto the orbital plane and transversal) is presented in the Fig. 2.

If initial inclination is sufficiently small then transfer can consist of unique acceleration or braking phase.

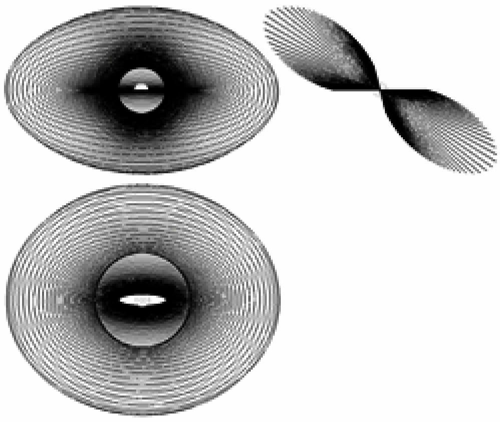

Fig. 3. Projections of minimum-time trajectory from circular orbit h =15000 km, i = 75° into the GEO (C-solution)

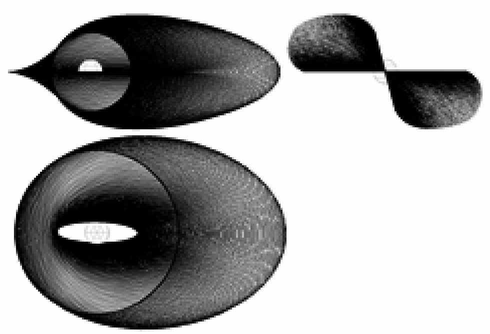

Fig. 4. Projections of minimum-time trajectory from circular orbit h =15000 km, i = 75° into the GEO (E-solution)

Let us denote the considered solution, which is characterized by zero eccentricity and equality ***J*** = 0° or ***J*** = 180° for averaged problem, as C-solution. Projections of typical C-trajectory are presented in the Fig. 3.

It was found another optimal solution (E-solution) when initial inclination is greater than critical one. The thrust vector position is not constrained by a local horizon plane on the averaged E-solution, therefore the eccentricity is nonzero on the trajectory. The projections of typical E-trajectory are presented in the Fig. 4. The dependencies of angles ***J*** and ***y*** versus time and argument of latitudes u on this trajectory are presented in the Fig. 5.

Typical phases of E-trajectory are following:

1. The acceleration-braking phase (acceleration in the pericentre vicinity and braking in the apocenter vicinity);
2. The pure acceleration phase;
3. The braking-acceleration phase (braking in the pericentre vicinity and acceleration in the apocenter vicinity).

Fig. 6 presents dependency of the maximal eccentricity, which is reached during the transfer, with respect to initial inclination. The initial altitude is 15000 km. E- and C-solutions are merged at the critical initial inclination 47.3°, and maximal eccentricity on the E-trajectory increases when initial inclination increases.

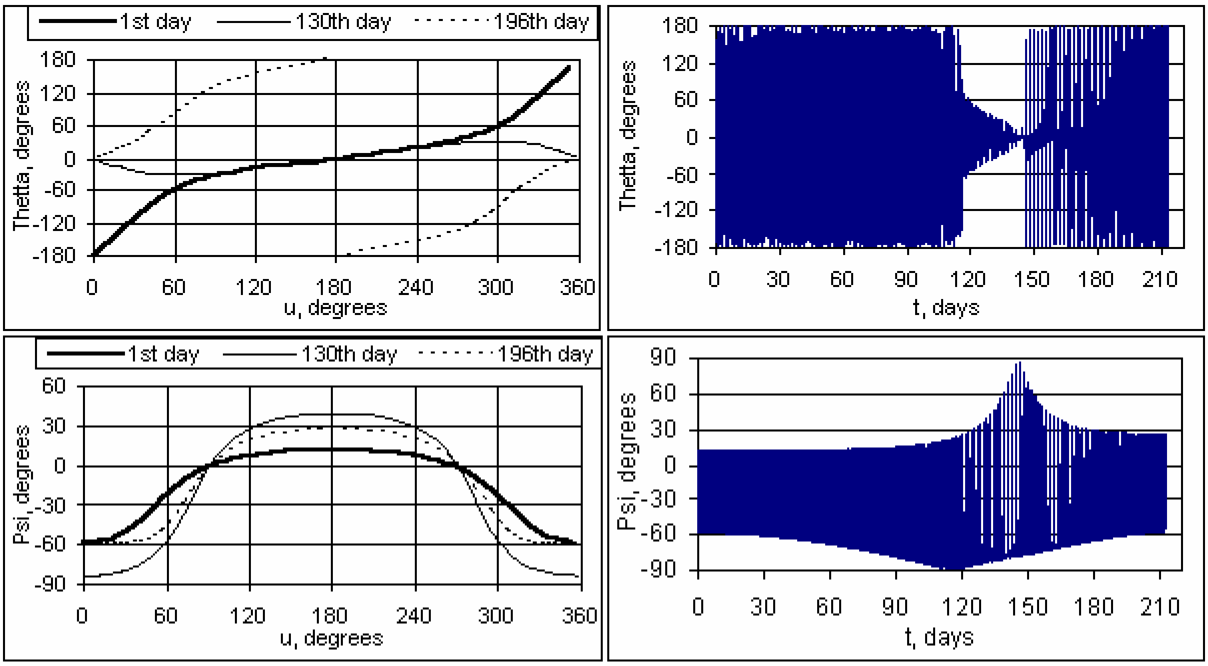

Fig. 5. Dependency of angles ϑ and ψ vs. time and argument of latitude for minimum-time transfer from circular orbit h = 15000 km, i = 75° into the GEO (E-solution)

The dependency of the ratio of maximal geocentric distance to the initial radius versus initial inclination is presented in the Fig. 7. In case of large initial inclination, the decreasing of pericentre radius on the initial phase of E-trajectory can take place.

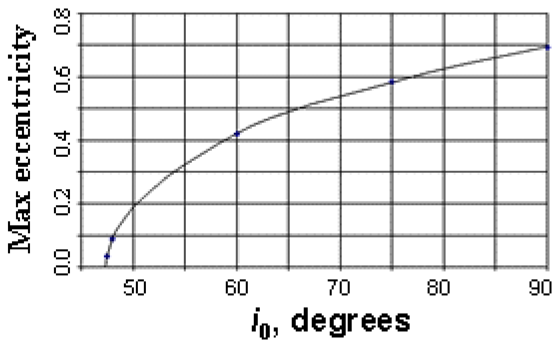

Fig. 6. Maximal eccentricity vs. initial inclination on the E-solution

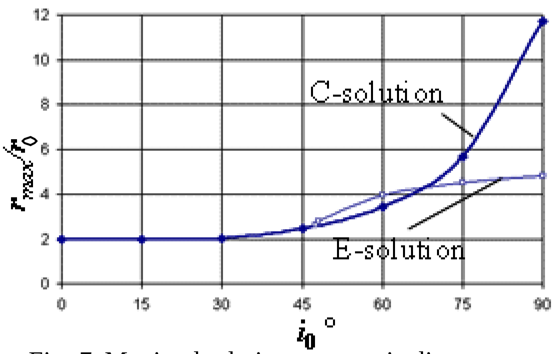

Fig. 7. Maximal relative geocentric distance vs. initial inclination on the E-solution

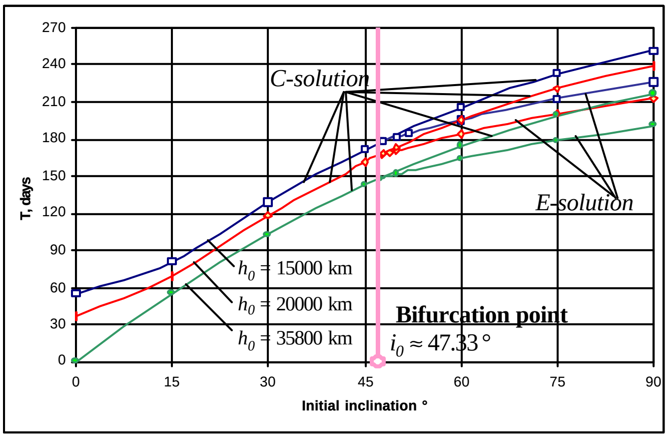

Fig. 8. Transfer duration vs. altitude and inclination of initial orbit (minimum-time problem)

The required increment of characteristic velocity on the E-trajectory is less than one on the C-trajectory. For minimum-time problem it corresponds to smaller transfer duration. Dependency of transfer duration versus initial inclination for C- and E-trajectories is presented in the Fig. 8.

Thus, if initial inclination is less than critical one, then C-trajectory is globally optimal, otherwise E-trajectory is globally optimal. Fig. 9 presents dependency of required characteristic velocity consumption with respect to initial inclination and initial altitude for globally optimal solution.

Advantage of globally optimal control in comparison with rely optimal control is presented in the Fig. 10. The improvement does not exceed 4% if initial inclination is less than critical, and it can be greater than 15% otherwise.

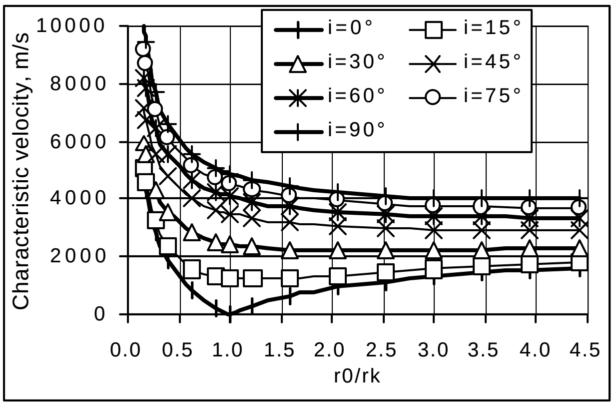

Fig. 9. Characteristic velocity vs. altitude and inclination of initial orbit

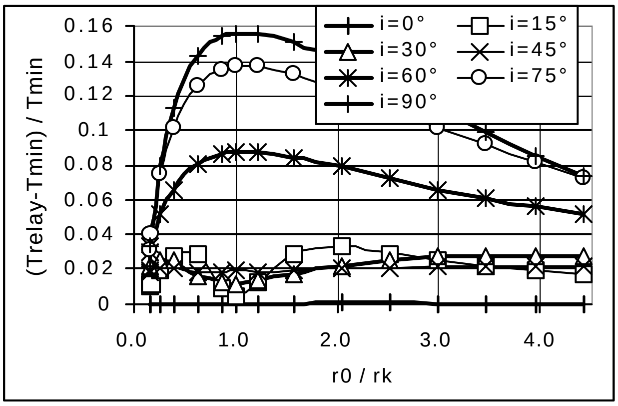

Fig. 10. Advantage of globally-optimal solution in comparison with optimal rely solution

Usage of minimum-propellant control allows essentially to increase final mass of spacecraft at the expense of increased transfer duration. Fig. 11 presents dependency of characteristic velocity, which is required for transfer from initial circular orbit having inclination 90° into GEO, versus transfer duration. The dashed line corresponds to the minimum-time problem for varied initial altitudes. Thick line corresponds to the minimum-propellant problem for initial altitude 30000 km, and thin line corresponds to the minimum-propellant problem for initial altitude 15000 km.

Maximal geocentric distance during transfer could be essentially greater than GEO radius in case of large initial inclination. The maximal geocentric radius monotonically decreases on the C-trajectories when the transfer duration increases. On the contrary, in case of E-trajectory, the maximal geocentric radius has a minimum at the transfer duration close to minimal one (Fig. 12).

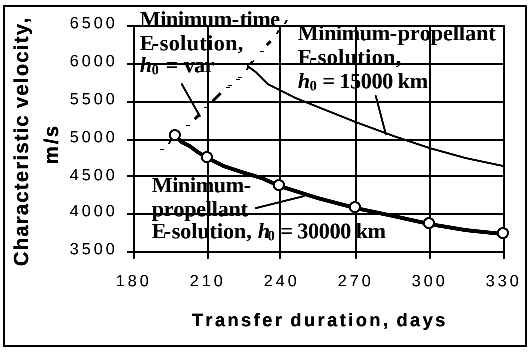

Fig. 11. Minimum-propellant transfers

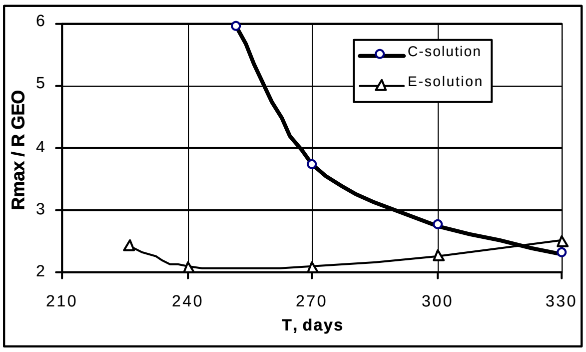

Fig. 12. Ratio of maximal geocentric distance to the GEO radius for transfer from initial circular orbit i=90°, h=15000 km into GEO

7.2 - 3D TRANSFER FROM AN ELLIPTICAL ORBIT INTO GEO.

C- and E-transfers between circular non-coplanar orbits generates corresponding solutions for transfer between non-coplanar elliptical and circular orbits. In this case, of coarse, the eccentricity and angle J are nonzero on the averaged C-solution. Qualitative difference of C-solution from E-solution consists in the eccentricity behavior. The maximal eccentricity at the C-trajectory never exceeds initial eccentricity, and, as contrary, the maximal eccentricity on the E-trajectory typically greater then initial eccentricity. If initial inclination is large enough, the apocenter and pericentre can trade its places on the C-trajectory (i.e. argument of pericentre can change from 0° to 180° or vice versa). An examples of C- and E-trajectories are presented in the Fig. 13.

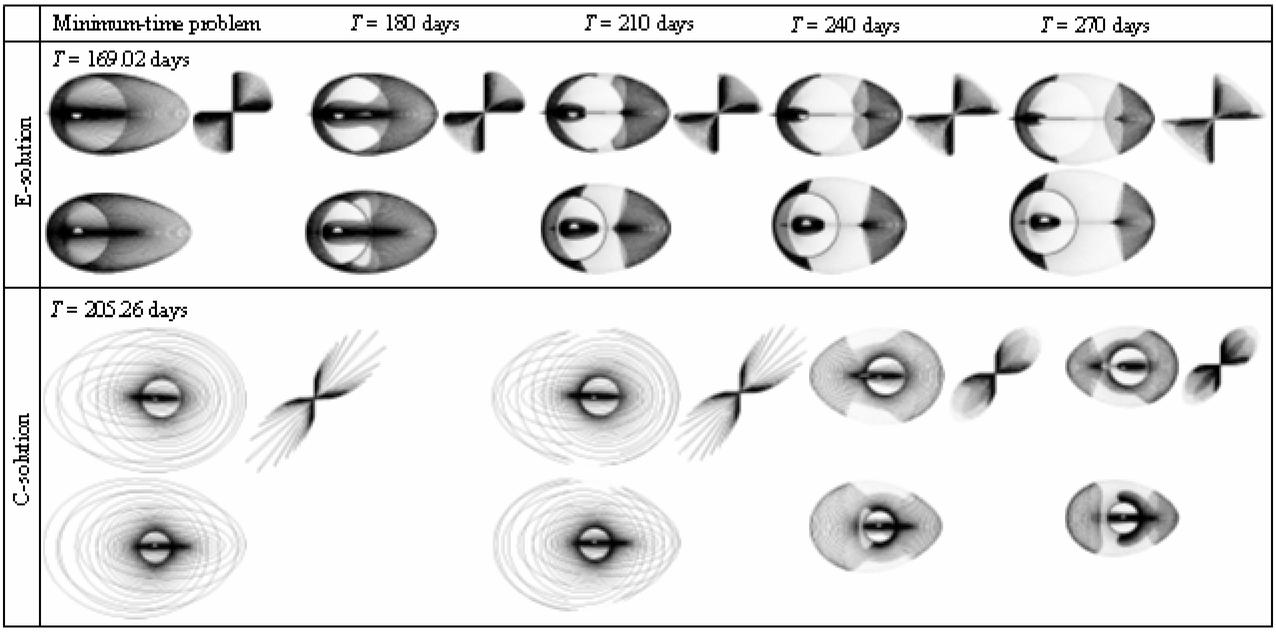

Fig. 13. Optimal transfer from the initial elliptical orbit h_α=60000 km, h_π=30000 km, i=90° into the GEO.
Upper row – E-trajectories, lower row – C-trajectories.
Left column – minimum-time problem, the rest columns – minimum-propellant problem.

Fig. 14 presents evolution of main orbital parameters on the minimum-time trajectory (initial pericentre altitude 30000 km, initial apocentre altitude 60000 km, initial inclination 90°).

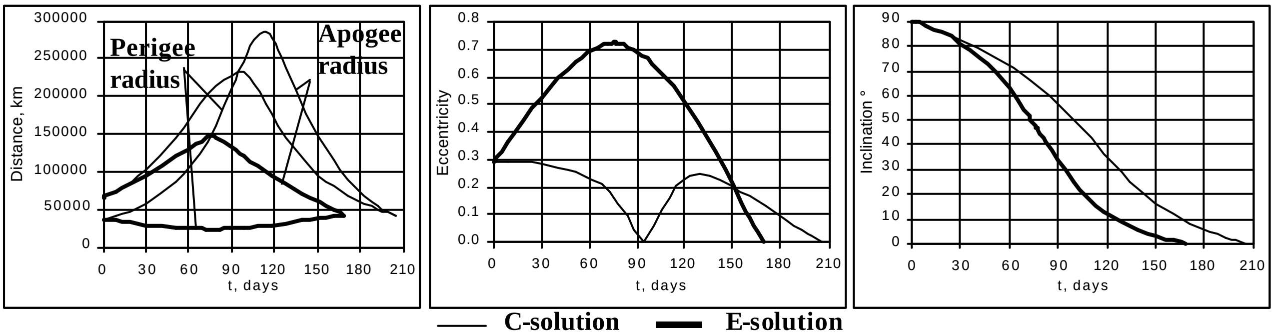

Fig. 14. Orbital evolution during the minimum-time transfer from the initial orbit i=90°, h_π=30000 km, h_α=60000 km into the GEO

The minimum-time problem was studied the most detailed. In particularity, there was carried out the series of computation of optimal trajectories for initial orbits having parameters given in the 3D-grid of pericentre altitudes, apocenter altitudes, and inclinations. Fig. 15 presents some results of these computations.

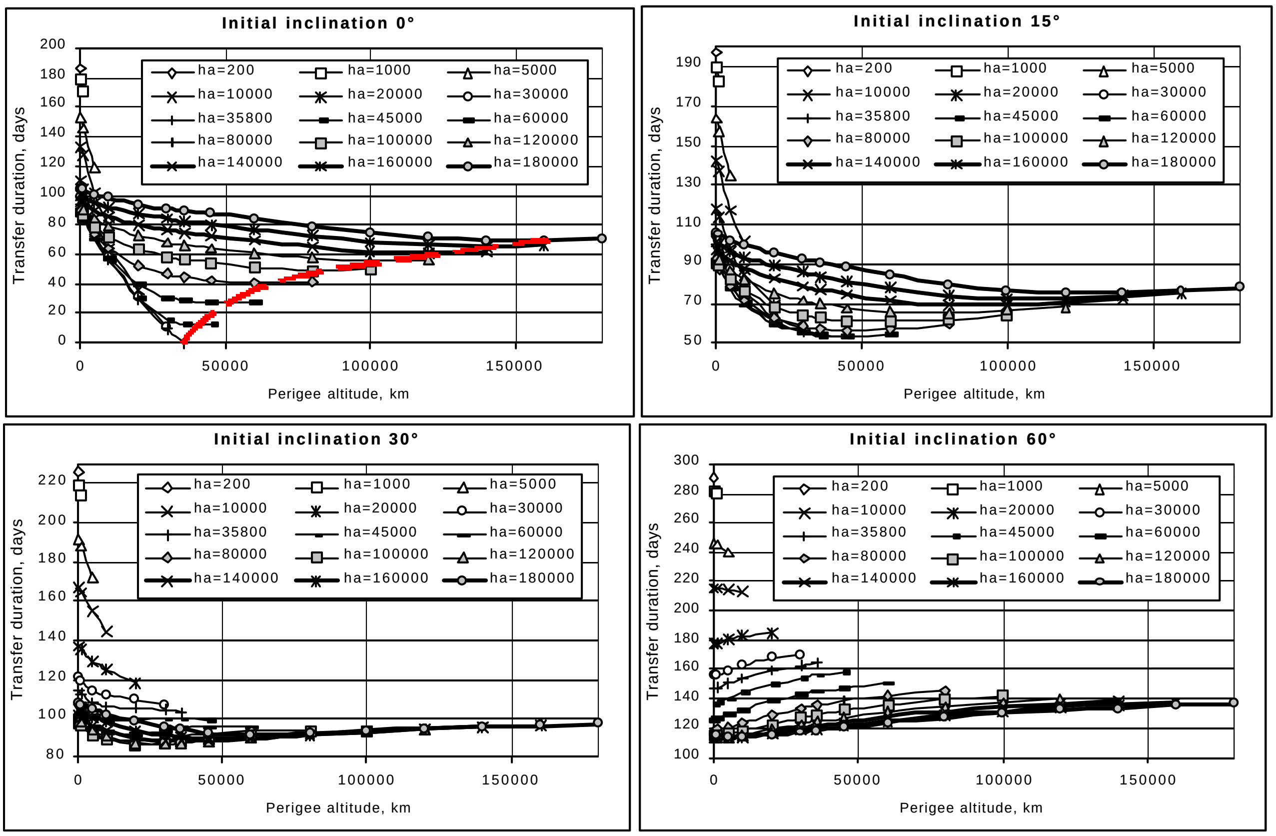

Fig. 15. Transfer duration vs. perigee altitude, apogee altitude and inclination of initial orbit

At first, it was found that initial inclination for transfer from the elliptical orbit into the GEO remains invariable - about 47.3°. As before, the E-solution is preferable inside its region of existence. Therefore, the presented results correspond to C-solution if initial inclination is less than critical one, and it corresponds to E-solution otherwise. Fig. 15 presents curves corresponding to optimal transfers from the initial orbit having fixed inclination, fixed apocenter altitude, and varied pericentre altitude. If initial inclination is less than critical one and initial apocenter altitude less than GEO altitude, then transfer durations decreases when pericentre altitude increases. If initial inclination is less than critical one but initial apocenter altitude is greater than GEO altitude, then an initial pericentre altitude exists, which corresponds to the minimal transfer duration (and minimal required increment of characteristic velocity). Let us call initial orbit, having such pericentre altitude, as the π-optimal orbit. The dashed line in the Fig. 15 corresponds to transfer from the π-optimal orbit having zero inclination into the GEO. When initial inclination increases, the optimal initial pericentre altitude decreases. When initial inclination becomes greater than critical one, it take place the qualitative reconstruction of dependency of transfer duration versus parameters of initial orbit. In this case, when initial apocenter altitude less than ~15000 km and initial pericentre altitude increases, the transfer duration decreases. If initial apocenter altitude greater than ~15000 km and initial pericentre altitude increases, the transfer duration monotonically increases.

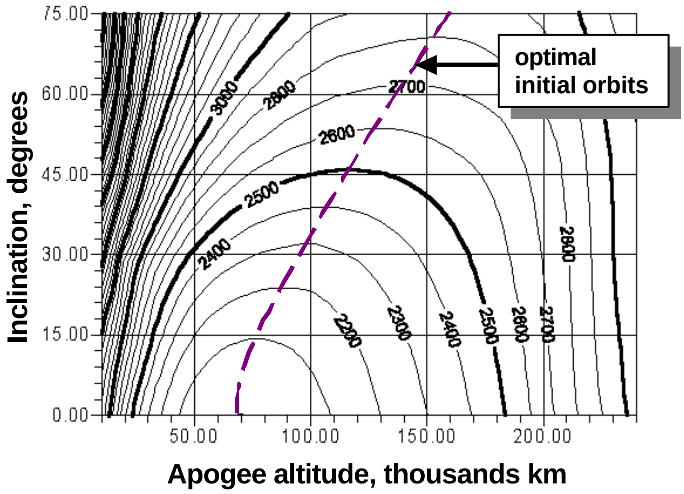

Fig. 16. Characteristic velocity, m/s, required for transfer from inclined elliptical orbits to GEO, versus apogee altitude and inclination of initial orbit. Initial perigee altitude is 250 km, specific impulse 1500 s, final thrust acceleration 0.34227 mm/s^2.

Fig. 16 presents contour plot of the required characteristic velocity for the minimum-time transfer from the high-elliptical initial orbit, having fixed pericentre altitude, into the GEO. The "optimal" initial apocenter altitude exists for each initial inclination (dashed line in the Fig. 16). Initial orbit, having the "optimal" apocenter altitude requires minimal characteristic velocity for given initial inclination. Let call such kind of "optimal" orbit as α-optimal orbit. If initial inclination equals to 0° then optimal initial apocenter altitude equals to ~70000 km, if initial inclination is 75° then optimal initial apocenter altitude is ~160000 km.

Line of optimal initial apocenter altitude divides parametric plane (initial apocenter altitude – initial inclination) into the regions having different structure of optimal control and different type of orbital evolution. There were found 3 kinds of the optimal transfers.

If initial apocenter altitude is low enough (the region on the left of dashed line in the Fig. 16) then minimum-time thrust steering includes up to 3 phases (the optimal transfer of the 1st kind). The first phase (it can be excluded when initial apocenter altitude is large enough) corresponds to the acceleration during complete orbit except for apocenter vicinity (Fig. 17). At the apocenter vicinity it take place the braking trajectory arc, which partially compensates the pericentre altitude increasing due to acceleration at the rest part of orbit. Extremal absolute magnitudes of angle y take place at the apocenter and pericentre crossing. The maximal apogean angle y is increases from the initial magnitude up to 90° during the first phase. The minimal angle y (at the pericentre) remains roughly invariable and its absolute magnitude is essentially less than apogean one. Eccentricity increases monotonically and it reaches its maximum at the end of first phase. The second phase

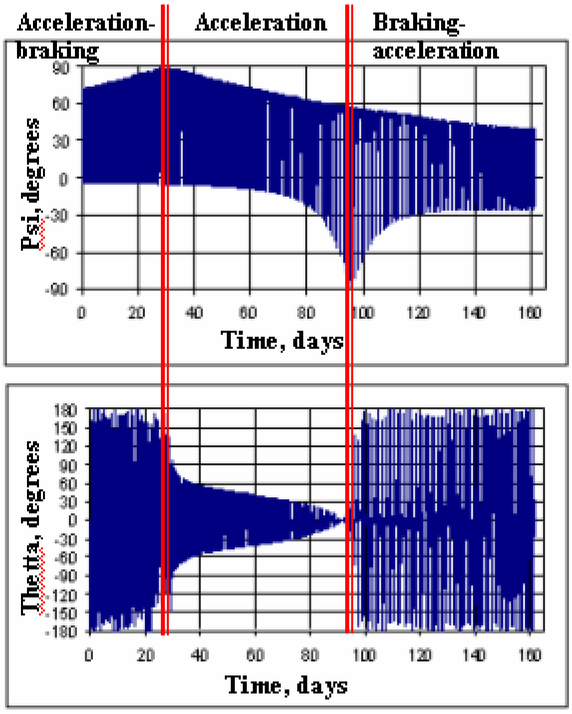

Fig. 17. Thrust steering on the optimal transfer of the 1st kind.

corresponds to the acceleration during complete orbit. Maximal angle y (at the apocenter) decreases monotonically, and absolute magnitude of the minimal angle y (at the pericentre) increases and reaches 90° at the end of this phase. The third phase corresponds to the acceleration at the apocenter vicinity and to the braking at the pericentre vicinity. As result, apocenter altitude decreases and pericentre altitude increases. Absolute magnitudes of extremal angles y (at the apocenter and pericentre) decrease, the absolute magnitude of apogean angle y becomes greater than one at the pericentre as early as at the beginning of 3rd phase. The maximal eccentricity take place at the bound of 1st and 2nd phases during the optimal transfer of the 1st kind. The maximal apocenter altitude take place at the bound of 2nd and 3rd phases. The semimajor axis has maximum during the transfer too. Averaged inclination monotonically decreases for all kinds of optimal transfers, of course.

The 1st phase duration decreases when initial inclination decreases. This phase vanishes at the some initial inclination. Then it decreases the duration of the 2nd phase. The 2nd phase vanishes when initial orbit becomes the α-optimal orbit.

Optimal transfer of the 2nd kind take place when initial orbit is α-optimal orbit (dashed line in the Fig. 16). Corresponding trajectory consists of unique phase having stable structure of thrust steering. It take place braking at the pericentre vicinity to decrease apocenter altitude and the acceleration take place at the apocenter vicinity to increase pericentre altitude. The peak magnitudes of angle y take place at the apocenter and pericentre. Apogean angle y decreases monotonically from 90°. Absolute magnitude of angle y at the pericentre decreases monotonically too. Averaged inclination, semimajor axis, apocenter radius, and pericentre radius vary monotonically.

The optimal transfer of 3rd kind take place when initial apogee altitude greater than optimal one (the region on the right of dashed line in the Fig. 16). Optimal trajectory consists of 2 phases. The braking take place during complete orbit at the 1st phase. The thrust steering at the 2nd phase is analogously to the thrust steering at the optimal transfer of 2nd kind. Maximal absolute peak magnitudes of angle y take place at the bound of phases, the maximal apogean angle y reaches 90°. Averaged pericentre radius has minimum and averaged eccentricity has maximum at the bound of phases. Apocenter radius, semimajor axis, and inclination are decreases monotonically.

7.3 - SMART-1 TRAJECTORY OPTIMIZATION – COMPARISON WITH ESOC RESULTS

The trajectory optimization of SMART-1 spacecraft is considered. The initial orbit has following parameters: perigee radius 20000 km, apogee radius 58068 km, inclination 6.655°, right ascension of ascending node 244.21°, and argument of perigee 200.23°. The parameters of the final orbit are following: apogee radius 219400 km, inclination 5.49°, right ascension of ascending node 0.25°, argument of perigee 79.66°. The final perigee radius is free. Initial spacecraft mass equals to 325.966 kg, transfer duration is fixed and equals to 284 days [4]. The electric propulsion provides thrust 45.82 mN and exhaust velocity 14674 m/s.

The results of carried out in the [4] optimization are following: final spacecraft mass equals to 303.9 kg and final perigee radius equals to ~ 26500 km. Optimization using considered in this paper techniques led to the slightly different results: final spacecraft mass equals to 303.6 kg and final perigee radius equals to ~24500 km. The projections of both trajectories onto the equatorial plane are presented in the Fig. 18..

Analysis of obtained results shows that compared trajectories are slightly differed by placement of burning arcs, have differences in the thrust steering, and they have slightly different orbital evolution. In addition, optimal trajectory, which is computed based on presented here techniques, has one orbit having two burning arcs (in contrary with optimal trajectory from [4], see Fig. 19).

Most likely, a little differences in the results (less then 0.1% of the propellant consumption) is explained by following reason: considered trajectories belong to different extremal solutions, which are consist of different number of complete revolutions around the Earth. In this connection, the open problem of computation the minimum-propellant trajectory, having fixed number of complete orbits, is actual.

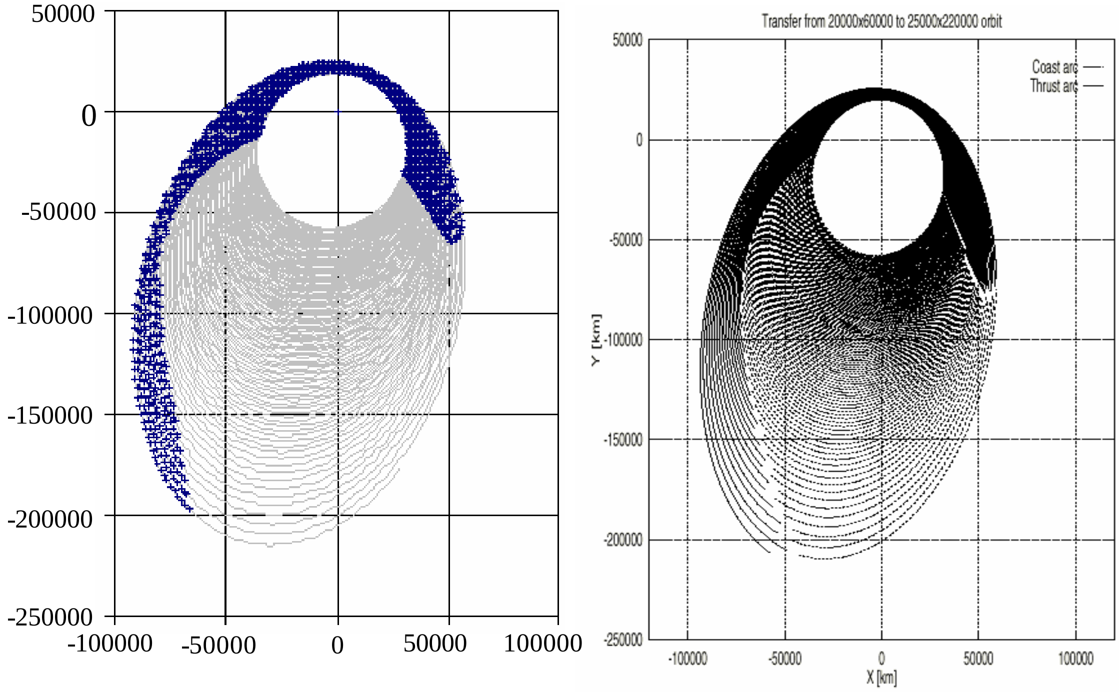

V. Petukhov

J.L. Cano & R. Jehn [4]

Fig. 18. Optimal trajectories comparison

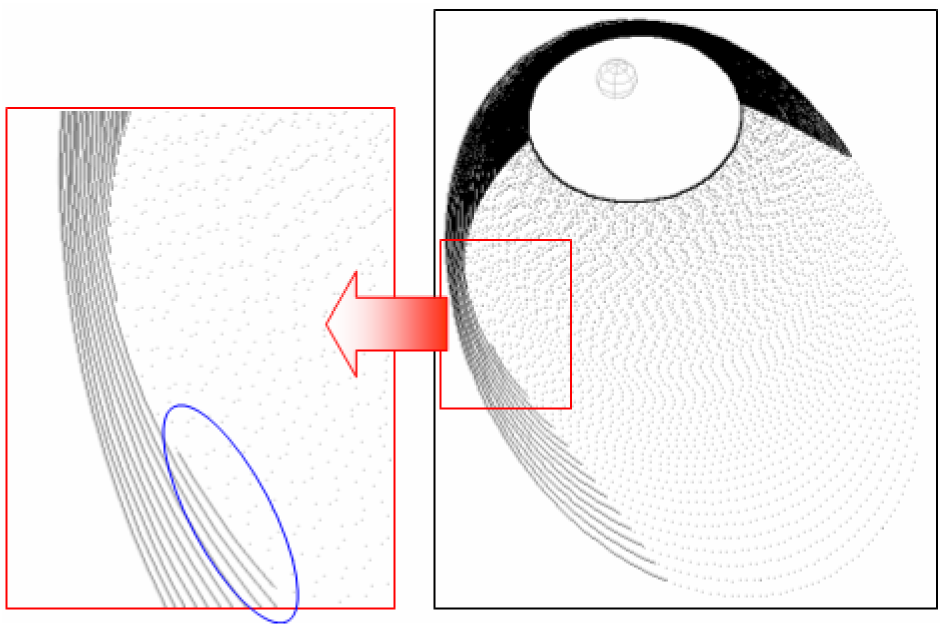

Fig. 19. Optimal trajectory of SMART-1 spacecraft

7.4 - COMPARISON WITH NON-AVERAGED OPTIMAL SOLUTION

One non-averaged minimum-time solution is presented in the paper [15]. There was considered the transfer from the elliptical orbit having semi-latus rectum 11625 km, eccentricity 0.75, and inclination 7° into the GEO. The spacecraft has initial mass 1500 kg, thrust 0.2 N, specific impulse 1994.75 s. There was found in [15] the minimal transfer time equals to 177.7375 days.

This problem was solved using presented in this paper techniques. The computed transfer time equals to 177.360 days. So, the relative difference between non-averaged [15] and averaged solution is ~0.2%. The averaged solution (namely, transfer duration and initial values of adjoints) was used to simulate spacecraft motion within non-averaged problem. The initial value of variable, adjoint to true longitude F, was assumed to be zero. The residuals at the right bound of the simulated trajectory was found following: Δe=0.0011, Δi=0.0030°, Δr_α=1734 m, Δr_π=-89826 m. So maximal error due to averaging technique take place for perigee radius. This error is ~0.2% too.

8 - CONCLUSION

Considered techniques allow to optimize efficiently the multirevolutional transfers between non-coplanar elliptical orbits. The continuation method is most efficient for a minimum-time problem. Solution of this problem is used as initial approximation for a minimum-propellant problem solving by a modified newton method.

The two types of optimal transfers from an inclined initial orbit into the GEO were found. The critical inclination was found. This inclination divides parametric space of the optimal control problem into the 2 regions. The unique type of optimal transfer (C-solution) exists in the one of these region and two types of optimal transfers (C- and E-solution) exist in another region. The structure of optimal thrust steering and orbital evolution for minimum-time problem were analyzed. The 3 kinds of optimal thrust steering controls were found for E-trajectories.

9 - BIBLIOGRAPHY

[1] L.L. Sackett, H.L. Malchow, T.N. Edelbaum. Solar Electric Geocentric Transfer With Attitude Constraints: Analysis. NASA CR-134927, 1975.

[2] S. Geffroy. Generalisation des Techniques de Moyennation en Controle Optimal - Application aux Problemes de Transfert et Rendez-Vous Orbitaux a Poussee Faible, November 1997.

[3] J. Fourcade, S. Geffroy, R.Epenoy. An Averaging Optimal Control Tool for Low-Thrust Optimum-Time Transfers (http://logiciels.cnes.fr/MIPELEC/en/logiciel.htm)

[4] J.L. Cano, J. Schoenmaekers, R. Jehn, M. Hechler. SMART-1 Mission Analysis: Collection of Notes on the Moon Mission. S1-ESC-RP-5004, 1999.

[5] S.R. Olesen, R.M. Myers, C.A. Kluever C.A., J.P. Riehl, F.M. Curran. Advance Propulsion for Geostationary Orbit Insertion and North-South Station Keeping. Journal of Spacecraft and Rockets, Vol. 34, No. 1, January-February 1997.

[6] A.G. Schwer, U.M. Schottle, E. Messerschmid. Operational Impacts and Environmental Effects on Low-Thrust Transfer-Missions of Telecommunication Satellites. 46th International Astronautical Congress. IAF-95-S.3.10. Oslo, Norway, 1995.

[7] A. Spitzer. Novel Orbit Raising Strategy Makes Low Thrust Commercially Viable. 24th International Electric Propulsion Conference, IEPC 95-212, Moscow, Russia, 1995.

[8] A. Medvedev, V. Khatulev, V. Yuriev, V. Petukhov, M. Konstantinov. Combined flight profile to insert telecommunication satellite into geostationary orbit using "Rockot" light-weight class launch vehicle. 51st International Astronautical Congress. IAF-00-V.2.09, Rio de Janeiro, Brasilia, October 2-6, 2000.

[9] M.S. Konstantinov, G.G. Fedotov, V.G. Petukhov, et al. Electric Propulsion Mission to GEO Using Soyuz/Fregat Launch Vehicle. 52nd International Astronautical Congress. IAF-01-V.3.02, Toulouse, France, October 1-5, 2001.

[10] A. Medvedev, V. Khatulev, V. Yuriev, V. Petukhov, A. Zakharov. Lunar and Planetary Missions Using Rockot Launch Vehicle. IAA-L-0704P.

[11] V. Petukhov. Low-Thrust Trajectory Optimization. Presentation at the seminar on Space Flight Mechanics, Control, and Information Science of Space Research Institute (IKI), Moscow, June 14, 2000 (http://arc.iki.rssi.ru/seminar/200006/OLTTE2.ppt).

[12] V. Petukhov. One Numerical Method to Calculate Optimal Power-Limited Trajectories. Moscow, IEPC-95-221, 1995.

[13] T.M. Eneev, M.S. Konstantinov, V.A. Egorov, R.Z. Akhmetshin, G.B. Efimov, G.G. Fedotov, V.G. Petukhov. Some Methodical Problems of Low-Thrust Trajectory Optimization. Preprint of KIAM No. 110, Moscow, 1996.

[14] T.M. Eneev, M.S. Konstantinov, R.Z. Akhmetshin, G.B. Efimov, G.G. Fedotov, V.G. Petukhov. Mercury-to-Pluto Range Missions Using Solar-Nuclear Electric Propulsion. Preprint of KIAM No. 111, Moscow, 1996.

[15] J.B. Caillau, J. Gergaud, J. Noailles. 3D Geosynchronous Transfer of a Satellite: Continuation on the Thrust. 2001 (http://www.enseeiht.fr/~caillau/papers/jota01.pdf).